

# Novel Fast Neutron Counting Technology for Efficient Detection of Special Nuclear Materials

D. R. Beaulieu, D. Gorelikov, H. Klotzsch, P. de Rouffignac, K. Saadatmand,

K. Stenton, N. Sullivan\*, A.S. Tremsin

**Abstract**— Results from a fully independent thin film process for manufacturing non-lead glass Microchannel plate (MCP) detectors using nano-engineered thin films for both the resistive and emissive layers are presented. These novel MCP devices show high gain, less gain degradation with extracted charge, and greater pore to pore and plate to plate uniformity than has been possible with conventional lead glass structures. Extension of MCP to plastic substrates, for the purpose of fast neutron detection is disclosed and preliminary MCP functionality results are presented. Simulation results, predicting fast neutron detection performance for the plastic MCP device are presented and discussed

**Index Terms**—Atomic layer deposition, Microchannel plate, Neutron detectors, Thin film devices.

## I. INTRODUCTION

Compact, solid state Microchannel Plate (MCP) electron multipliers are used in a variety of applications including; astrophysical sensors, mass spectroscopy, synchrotron instrumentation, and image intensifiers. Recent advances in MCP readouts and their associated electronics allow 2-dimensional imaging of photon/ ion/ electron/ neutral particles with better than 10  $\mu\text{m}$  positional<sup>1</sup> and 20 ps timing resolution<sup>2</sup> and with background rates of less than 0.01 counts/cm<sup>2</sup>/s. However, state-of-the-art of MCP manufacturing has not advanced significantly since the mid-1970s, relying on mature but labor-intensive, fiber optic manufacturing technology. The MCP is typically manufactured using a glass multifiber draw (GMD) process. In the GMD process, individual composite fibers, consisting of an etchable core glass and an alkali lead silicate cladding glass, are formed by drawdown of a rod-in-tube preform. The rod-in-tube preforms are then packed together in a hexagonal or rectangular array. This array is then redrawn into hexagonal/rectangular multifiber bundles, which are stacked together and fused within a glass envelope to form a solid billet. The solid billet is then sliced, typically at a small angle of approximately 4°-15° from the normal to the fiber axes. Individual slices are then polished, forming a

thin plate. The soluble core glass is removed by a chemical etchant, resulting in an array of microscopic channels with channel densities of  $10^5$  - $10^7$  /cm<sup>2</sup>. Further chemical treatments, followed by a high temperature hydrogen reduction process, produces the resistive and emissive surface properties required for electron multiplication within the microscopic channels. Metal electrodes are thereafter deposited on the faces of the wafer. The hydrogen reduction step is critical for the operation of state-of-the-art MCP devices and determines both the resistive and the emissive properties of the continuous dynode. Lead cations in the near-surface region of the continuous glass dynode are chemically reduced, in a hydrogen atmosphere at temperatures of 350°-650° C, from the Pb<sup>2</sup> state to lower oxidation states with H<sub>2</sub>O as a reaction by-product. This process results in the development of significant electrical conductivity within a submicron distance to the surface of the reduced lead silicate glass (RLSG) dynode. The physical mechanism responsible for the conductivity is not well understood but is believed to be due to either an electron hopping mechanism via localized electronic states in the band gap or a tunneling mechanism between discontinuous islands of metallic lead within the RLSG film. The RLSG manufacturing technology is mature and results in the fabrication of relatively inexpensive and high performance devices. However, the RLSG manufacturing technology has certain undesirable limitations. For example, both electrical and electron emissive properties of RLSG dynodes are quite sensitive to the chemical and thermal history of the glass surface comprising the dynode. The multifiber drawdown technique requires that the core and cladding starting materials both be glasses with carefully chosen temperature-viscosity and thermal expansion properties. The fused billet must have properties suitable for wafering and finishing. The core material must be preferentially etched over the cladding with very high selectivity. In addition, the clad material must ultimately exhibit sufficient surface conductivity and secondary electron emission properties to function as a continuous dynode for electron multiplication. This set of constraints greatly limits both the range of materials suitable for manufacturing and the ability to optimize the performance characteristics for RLSG MCPs critically depend upon stringent control over complex, time-consuming, and labor-intensive manufacturing operations. Performance limitations include: gain amplitude

Manuscript received March 26, 2009. This work was supported in part by the U.S. Department of Defense under HR0011-05-9-0001 awarded by the Defense Advanced Research Projects Agency (DARPA).

N.T. Sullivan is with Arradance Inc., Sudbury, MA 01776 USA (phone/fax: 888-949-4441; e-mail: nsullivan@arradance.com).

and stability, count rate capabilities, maximum processing temperature, maximum operating temperature, background noise, reproducibility, size, shape, and heat dissipation in high-current devices.

Several attempts have been made to produce MCPs with more advanced, thin film processing, such as silicon micromachining<sup>3,4,5,6</sup> and lithographic etching/punching of anodic alumina<sup>7,8,9</sup> with limited success due to the complex film optimization required to achieve desired performance.

Significant advances in thin film deposition techniques, especially as relate to atomic layer deposition (ALD), make it possible to engineer thin, active films that bring performance and manufacturing improvements to the MCP. Most importantly for detection of special nuclear materials (SNMs), these thin film technologies enable MCP production from a wide range of substrate materials. By separating the manufacturing from lead glass materials technology, MCPs can be made from low atomic number materials, such as plastic, eliminating radioactive elements in the substrate (e.g. Rb and K) and resulting in a significant improvement in the dark count rate characteristics. Since the conduction and secondary electron emission layers of these novel MCPs are not determined by the substrate material, they can be individually tuned for a specific application. Further, the substrate can be optimized for a specific application and can itself form an active part of the detector.

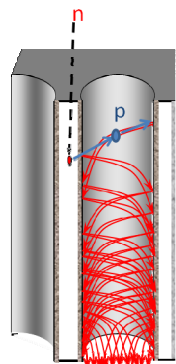


Figure 1: n-p recoil reaction in plastic MCP pore initiates an electron avalanche in the adjacent pore.

In the MCP-based device, as envisioned, neutron detection is accomplished through the conversion of incoming fast neutrons into a pulse of electrons, using the neutron-proton (n-p) recoil reaction within a hydrogen-rich, plastic microchannel substrate, as shown in Figure 1. The proton then excites secondary electrons, which are amplified by a factor of  $10^3$ - $10^6$ . Such high gain will allow event counting at very low input fluxes with very low background noise. The prototype MCP device produces an output that is readily registered by a large variety of available technologies. The core of this

technology is the thin film materials and low temperature processes used to functionalize hydrogen-rich plastic microchannel structures with conductive and high secondary electron (SE) emissive films enabling these high gain neutron detectors.

Advantages over existing passive neutron detection (He-3,  $^{10}\text{B}$ -doped MCPs) technologies lie in the capability for direct detection of fast neutrons, combined with intrinsic low gamma sensitivity. Thermal neutron detectors, when used in this application, require moderation of the fast neutrons, substantially reducing the event counting rates and effectively

destroying any energy or spatial information of the original fast neutron. The advantage of the proposed technology over the existing fast neutron detectors is: the direct conversion of fast neutron into a measurable electrical signal, high temporal and spatial resolution, the absence of readout noise and the complete lack of afterpulsing. State-of-the-art active interrogation systems rely on plastic or liquid scintillators for fast neutron detection, where neutrons are converted into a pulse of light and subsequently detected by a photomultiplier tube (PMT). The PMT sensitivity is tuned to match the spectral range of scintillation photons, typically in the visible range. The timing accuracy of neutron detection is limited by the scintillator decay time and by the intrinsic noise in the PMT, typically to values greater than 100 ns. Relatively long afterpulsing in scintillators also limits the maximum counting rate achievable in a given area. The process of fast neutron absorption, signal amplification and readout in the plastic MCP will take substantially less than 10 ns without the presence of delayed signals. In case of active interrogation, with a pulsed neutron or gamma beam, the high timing accuracy of neutron detection will enable high resolution determination of neutron energy, utilizing a time of flight method. Further, it may be possible to determine the SNM source location via the directional, active neutron irradiation. Active interrogation efficacy is also improved with the capability to discriminate prompt and delayed neutrons which can be an unambiguous indicator of the presence of SNM. The high timing resolution will also allow efficient discrimination between the neutrons generated in a fusion chain within SNM (as detected in a particular energy window) and the diffuse background radiation. Extending this methodology, it may also be possible to measure the spectral distribution of emitted neutrons. This technology will also enable high spatial resolution for each detected neutron, on the scale of few hundred micrometers, based upon the geometry of the plastic MCP.

## II. MCP EXPERIMENTAL RESULTS

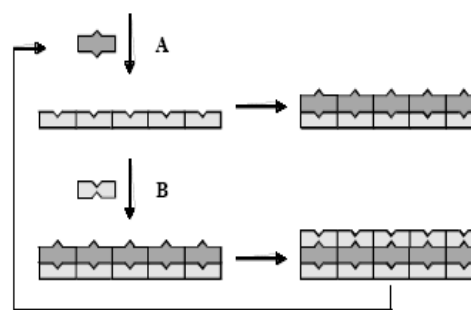


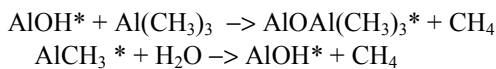
Fig 2: Reaction sequence for ALD

### A. ALD emissive and conductive films

ALD is a thin film growth technique that relies on two sequential, self-limiting surface reactions between gas-phase precursor molecules and a solid surface as illustrated in Figure 2. The surface is initially exposed to reactant A, which reacts

with initial surface sites. Following this, the products from the A sequence are purged and the surface is exposed to reactant B. This reaction regenerates the initial functional groups and prepares the surface for the next exposure to reactant A. The film is grown to the desired thickness by repeating this AB sequence. Since each reaction is self-limiting, line-of-sight deposition is not required and high aspect ratio structures and complex geometries can be conformally coated. Smooth, dense films result when the two reactions are allowed to go to completion. ALD techniques exist for depositing a variety of substances including oxides, nitrides, and metals. ALD has many important benefits over other more standard thin film deposition techniques such as chemical vapor deposition (CVD). During CVD, the surface is exposed to both reactants at the same time. This allows for gas-phase reactions, which can cause particle formation and poorly controlled growth. During ALD, only one reactant is present at a time so that only surface reactions occur. This insures smooth conformal films with atomic level control over growth. Additionally, ALD can be performed at temperatures well below typical CVD temperatures, thus allowing the coating of relatively fragile materials, such as polymers, without damage.

A typical ALD film deposition reaction cycle is that of Alumina,  $\text{Al}_2\text{O}_3$ . Such films are deposited using alternating exposures of trimethylaluminum ( $\text{Al}(\text{CH}_3)_3$ , TMA) and water. The chemistry of  $\text{Al}_2\text{O}_3$  ALD occurs via the following reaction, where the asterisk represents surface species



At a deposition temperature of 177 °C, the growth rate for  $\text{Al}_2\text{O}_3$  ALD is 1.2 Å/cycle and the typical cycle time is 12 seconds.  $\text{Al}_2\text{O}_3$  films grown by ALD techniques are insulating, amorphous and smooth.

#### B. ALD-based improvements of RLSG microchannel plates

Gain, lifetime and uniformity are the crucial parameters determining the ultimate performance of an MCP device. Although the processes of MCP ageing are not completely yet understood on the microscopic level, it is well known that the secondary electron emission properties of pore walls degrade with the extracted charge<sup>10</sup>. To stabilize the detector operation a time consuming process of electron scrubbing is performed before the MCP devices are delivered. Moreover, gain degradation limits the overall lifetime of the device since the gain compensation, by increasing the operating voltage, has its limits.

Modification of the emission properties of the existing glass microchannel plates was the first step towards fully nano-engineered conduction and emission films. A set of commercially available MCPs was used. Fig. 3 shows the gain of those MCPs measured before and after the treatment. The gain of treated microchannel plates was routinely measured to increase by a factor of 5x-10x for a variety of MCP geometries and initial gains. The gain saturation at high input currents did not change after treatment, as expected, and was measured to onset at usual ~10% of the strip current. Indeed, the current

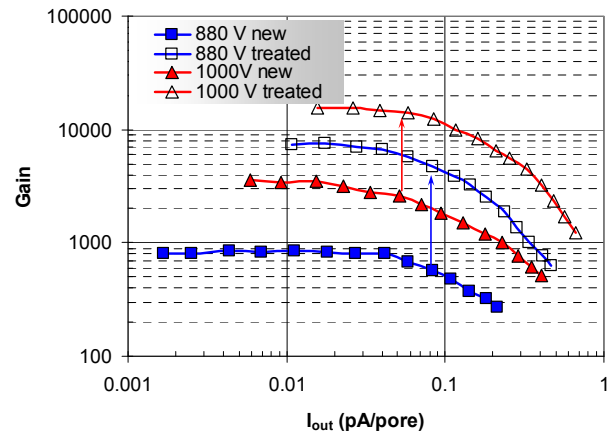


Fig. 3. Variation of commercial MCP gain measured as a function of output current. The gain is measured for a fresh MCP and after the MCP was treated with high secondary electron emission film. The MCP pores are 4.8  $\mu\text{m}$  in diameter, 18 mm active area, aspect ratio of ~50:1, plate resistance ~250  $\text{M}\Omega$ . The gain saturates at output currents ~10% of the strip current. The MCP is illuminated with a uniform flux of electrons.

saturation is determined by the ability of the pore to recharge and is mostly governed by the combined resistance of the pore conduction and emission layers. The tunneling of the charge into the emission layer was still the limiting factor for the count rate capabilities of the MCP treated with the emission layer. The output uniformity of the treated MCPs was also found to remain unchanged confirming the good spatial uniformity of the new treatment.

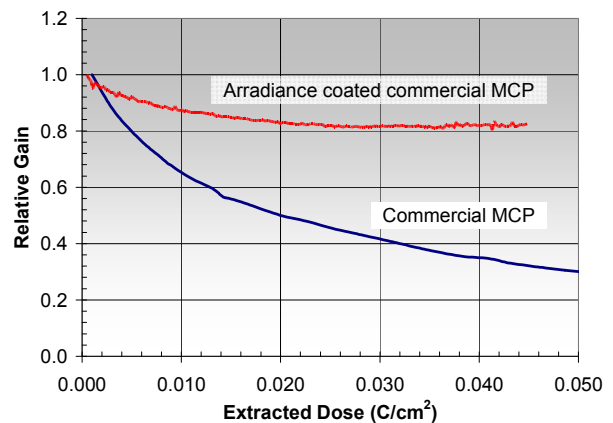


Fig. 4. The relative gain variation measured as a function of extracted charge (ageing curves). Two initially identical microchannel plates are measured: one as received from the manufacturer, while the other was treated for high secondary electron emission. 4.8  $\mu\text{m}$  pores,  $L/D=50:1$ ,  $R_{\text{MCP}}=100\text{-}200 \text{ M}\Omega$ . The scrubbing was performed at 880 V bias, the output current ~10-20% of strip current.

The gain degradation of the treated MCP was found to be substantially reduced, as shown in Fig. 4. The gain reached stable operation after 0.02 Coulombs/cm<sup>2</sup> was extracted at a typical output current equal to 10-20% of the strip current, while a similar pre-treated plate required 0.1 Coulombs/cm<sup>2</sup> charge extraction.

### C. MCPs with nano-engineered conduction and emission layers

The conduction and emission properties of the pore walls in commercial microchannel plates are determined by the composition of the lead glass. The natural extension of the work reported in the previous section was to engineer both

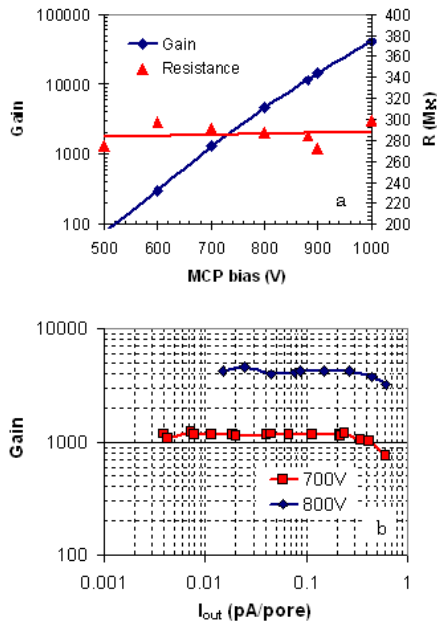


Fig. 5. (a) Resistance and gain of MCP with nano-engineered conduction and emission films. (b) MCP gain measured as a function of output current. Non-lead glass MCP substrate with 10  $\mu\text{m}$  pores, 18 mm active area, L/D=40:1 was coated with both conduction and emission films. Measurements are performed under uniform illumination of electrons.

conduction and emission layers. Since these films are very different in composition, thickness and functionality it is possible, in contrast to the lead glass process, to independently optimize the performance of each film. The resulting properties of these novel MCPs do not depend on the substrate type on which they are deposited on as long as the adhesion to the substrate is sufficient. Figs 5.a and 6.a show the measured resistance of the nano-engineered microchannel plates with two different types of geometry:  $\sim 5 \mu\text{m}$  and  $\sim 10 \mu\text{m}$  pore diameters. The resistivity of the conduction film was intentionally tuned in order to produce MCPs with target resistances of few hundred MΩ. Resistance was found to be stable at accelerating biases up to 1 kV and the thermal coefficient of resistance was comparable to standard values observed with standard lead glass MCPs. The same graphs show the measured gains under electron bombardment. The gain reached very high values of 40000 for a single stage 40:1 L/D device biased at 1000V. The gain saturation was observed to appear at output currents equal to  $\sim 10$ -30% of strip currents, as seen in Figs. 5.b and 6.b. The demonstrated deposition of both conduction and emission films on a non-lead glass substrate allows the separation of the electrical properties of the resulting MCP

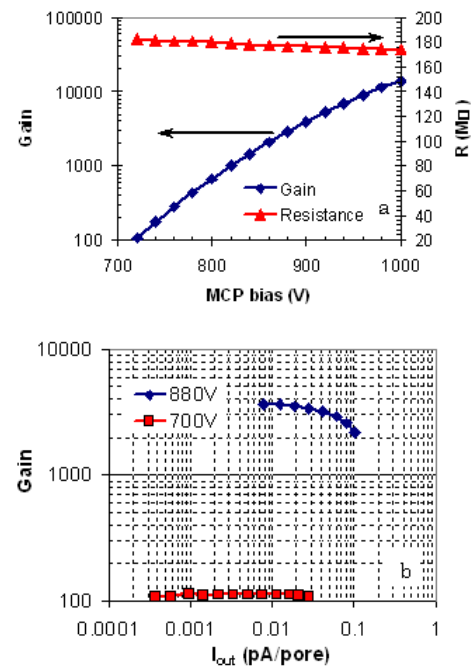


Fig. 6. (a) Resistance and gain of MCP with nano-engineered conduction and emission films. (b) MCP gain measured as a function of output current. Unfired glass MCP substrate with 4.8  $\mu\text{m}$  pores, 18 mm active area, L/D=50:1 was coated with both conduction and emission films. Measurements are performed under uniform illumination of electrons.

from the substrate material, enabling MCP production from a wide range of substrate materials and geometries, including micromachined structures, bulk conductive, high temperature compatible and plastic substrates.

### D. Fast Neutron detection with MCPs

Neutrons and gamma rays, both long-range neutral entities, cannot be detected directly. However, neutrons can transfer their energy to short range charged particles such as protons and alpha particles. These secondary particles can be used to produce measurable electrical signals. Hydrogen containing materials provide the highest efficiency for the neutron-proton (n-p) recoil reaction. Fast neutrons, interacting with a specialized plastic substrate, will generate recoil protons (Fig. 1), which will be used to initiate an electron avalanche within the adjacent MCP pores that have been functionalized by the emissive and conductive thin films. Once the secondary electrons are produced in the pore, the process of amplification and detection is identical to the standard operation of the MCP device as implemented in low flux applications. In most solid neutron detection schemes, P1 increases as the density of absorber nuclei increases—but usually at the expense of a corresponding decrease in P2; due to the rather limited range (several microns) of the proton recoil. In sharp contrast MCP neutron detection is highly unique, in that its microscopic structure can circumvent this problem, through use of micron-thin walls alternating with open channels (Fig. 1).

The neutron detection efficiency  $Q_n$  of a plastic fast neutron MCP detector is given by the product of three terms,

$$Q_n = P1 * P2 * P3 \quad (1)$$

where P1 is the fraction of incident neutrons which recoiled on a hydrogen atom in the MCP structure, P2 is the fraction of those interactions that generate an electron avalanche within an MCP channel, and P3 is the fraction of avalanches that are registered by the readout electronics system. For conventional MCP geometries the detection efficiency is largely determined by the first two terms P1 and P2 as the probability P3 is nearly unity. P1 is determined by the probability of neutron interaction through the neutron-proton recoil within the bulk MCP plastic composition which is a function of the H content of the material. Neutron interaction with the other elemental components of the plastic (Carbon and Oxygen) are not considered due to their negligible contribution to the detected signal. The second term P2 addresses the escape into an open channel of the recoil proton. We assume that, once created, an electron avalanche always yields a detectable electron pulse, implying  $P3 \sim 1$ .

The probability that a neutron is absorbed inside an MCP is given by:

$$P_1 = 1 - \exp(-N_H \sigma_n L_{eff})$$

where  $N_H$  is the number of H atoms per unit volume of the MCP structure,  $\sigma_n$  is the cross-section for the n-p recoil reaction, and  $L_{eff}$  is the effective path length of a neutron inside the MCP. It is well known that  $\sigma_n$  is a function of neutron energy, is generally inversely proportional to the neutron velocity<sup>11</sup>, and for H is essentially structureless over the range of neutron energies of interest. For neutrons having an energy 1 MeV, the cross-section is 4.3b. Our first plastic MCP manufactures from PMMA substrates contains approximately 7-wt% H resulting in the (n-p) recoil probability P1 within 5 mm thick plate on the order of several percent.

The probability, P2, that a proton once liberated will escape into the MCP pore is calculated using the inter-pore geometry and Monte Carlo methods to estimate the proton-substrate interactions.

Simulation results for P1\*P2 combined probabilities for a 5mm thick MCP, are shown in Figure 7. As can be seen, the total probability is a strong function of the MCP pore wall thickness, with a maximum for 2 MeV neutrons at  $\sim 10 \mu\text{m}$  wall thickness and for 10 MeV neutrons at  $\sim 30 \mu\text{m}$  walls (and  $50 \mu\text{m}$  pores in both cases), both of which are well within the present, plastic MCP manufacturing capability.

The timing resolution of this fast neutron detection technology, is expected to be better than 10ns, limited only by the depth of neutron absorption within the MCP and transit time spread of the electron avalanche, which varies between  $\sim 50$  ps and few ns for the considered MCP geometries. High detection efficiency for fast neutrons can be achieved since, the probability of neutron recoil in the plastic, coupled with the proton escape and secondary electron generation probabilities are sufficiently high to allow for better than 1% neutron detection efficiency.

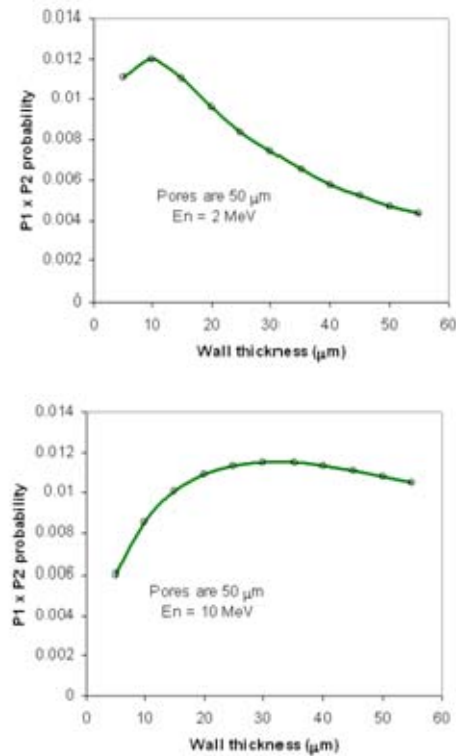


Figure 7: P1\*P2 for 5mm PMMA MCP

Successful passive SNM detection requires high efficiency in the presence of large background gamma radiation. The intrinsic sensitivity of the plastic MCPs to gamma photons, expected to be below the  $10^{-4}$  level, will be substantially lower than the sensitivity of standard glass MCPs ( $10^{-2}$ )<sup>11</sup> that contain a large fraction of heavy lead atoms. A coincidence technique, using consecutive detectors, can also be implemented to further improve gamma background discrimination, within a projected 50 ns coincidence window. Directionality determination is also possible whereby the consecutive detectors device operation is monitored in both “directions”. More advanced “imaging” capabilities, taking advantage of the potential of the MCP structure to achieve high spatial resolution, may be achieved through the use of coded aperture approaches as used in the imaging of hard X-ray and Gamma ray radiation. Demonstration of the expected high level of performance of the proposed detector may allow future development of more advanced detector configurations having the ability to determine neutron energy, directionality, and SNM source location with a large format.

#### E. Plastic MCP performance

Prototype plastic MCP devices, manufactured with a modified fiber optic multi-draw process<sup>12</sup> using Polymethylmethacrylate (PMMA) have been procured and functionalized using the low temperature ALD conductive and emissive film processes. The initial prototype devices are approximately 2mm thick with  $50 \mu\text{m}$  pores with  $20 \mu\text{m}$  sidewall ( $70 \mu\text{m}$  pitch). The devices contain approximately 10,000 pores within the active region. A representative SEM

image is shown in Figure 8. While the pore uniformity is not acceptable, the overall geometry and density are sufficient to test the basic MCP functionality of the films on the plastic substrate. Performance results are shown in Figure 9 for the

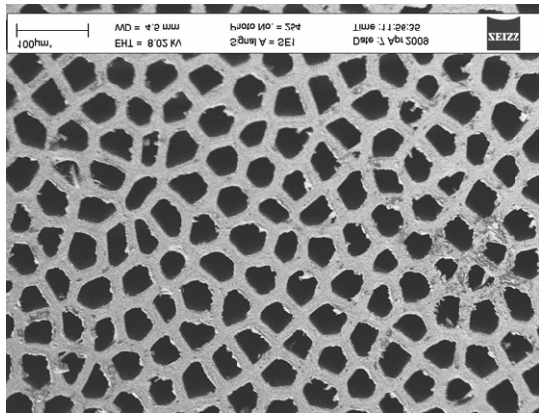


Figure 8: SEM image of the first PMMA MCP substrate

first ever, plastic MCP. The device output vs. bias agrees well with expected values, based upon simulation, for the pore geometries of the substrate.

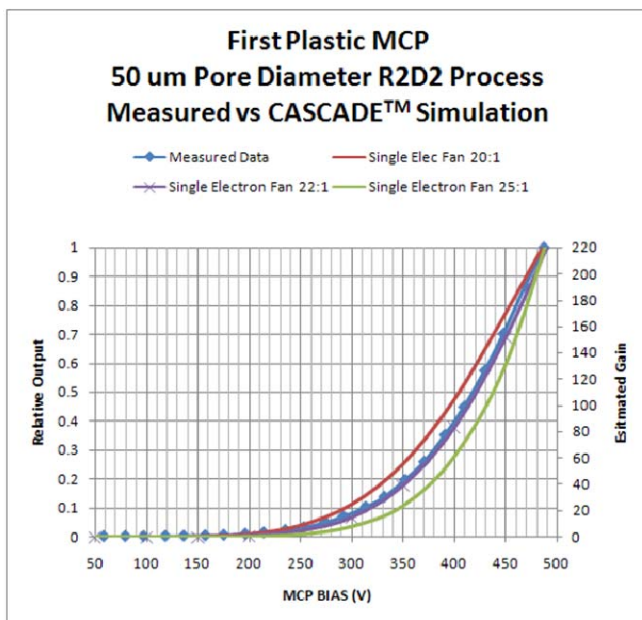


Figure 9: Predicted and measured gain of first Plastic MCP as a function of acceleration bias. Good agreement between the predicted and experimental values is observed, enabling future optimization of the device performance through computer simulation.

The timing resolution of this fast neutron detection technology will be limited only by the depth of neutron absorption and the transit time spread of an electron avalanche within the pore(s). It is expected that this technology should be capable of timing resolution of better than 10ns. The detection efficiency of the plastic MCP should reach levels as high as

few percent for fast 1-10 MeV neutrons. The probability of neutron recoil in the plastic selected for study is shown in Fig. 2. While it is feasible to produce 10 mm thick MCPs with 100 µm pores (aspect ratio L/D=100:1), our initial prototypes will concentrate on MCPs 3-5 mm thick with 100 µm pores, which (Fig 2) will provide reasonable efficiency in a testable configuration.

The time difference between detected events on each of the two detectors and the spatial coordinates of these events will allow for determination of the energy of the scattered neutron that is detected, via an n-p recoil reaction, in the second detector. The two consecutive detectors can be placed in a very close distance of only few cm from each other. The spectrum of fission energies is well known for given materials and therefore the coincidence window can be selected. Using the Watt distribution for fast neutrons (1MeV peak, 2 MeV mean energy), indicates that fission neutron energies can be expected to range between 0.1 MeV and 5 MeV. For a 10 cm gap between the detectors (Fig 10) the flight time will be between 3 and 23 ns for non-scattered neutron. Taking into account  $\sim E_n/2$  factor (energy corresponding to the flight of neutron with half of its initial energy), the second particle should be registered by the second detector within 50 ns of the first event. Therefore, a narrow coincidence window of  $\sim 50$  ns may be a reasonable value for the proposed gamma rejection technique, well within the expected timing resolution of the detector ( $< 10$ ns). Thus, most of the background events will not meet the coincidence criteria and will be rejected.

Extensions of the coincidence technique can also be envisioned. For example, device operation can occur in both “directions” e.g. events which had  $\Delta T > 0$  will originate from detector 1 (Fig 10), while  $\Delta T < 0$  corresponds to neutrons arriving from detector 2. This will provide some neutron directionality within the initial, proposed device configuration. More complex configurations with multiple detector (Fig 11) orientations will further specify neutron source location. More advanced “imaging” capabilities may be achieved through the use of coded aperture approaches as used in the imaging of hard X-ray and Gamma ray radiation.

### III. CONCLUSION

Functionalizing hydrogen-rich, plastic microchannel plate substrates with Arradance thin film technology will produce high gain, fast neutron sensitive electron multipliers. The neutron-proton (n-p) recoil reaction, occurring within the innovative plastic MCP device, is used to convert incoming fast neutrons into a pulse of  $10^3$ - $10^6$  electrons, providing an efficient, low noise means for passive and active SNM detection. Demonstration of the expected high level of performance of the proposed detector will allow for implementation of more advanced detector configurations which may result in significant gamma discrimination, capability to determine neutron energy, directionality, and even SNM source location through time of flight techniques

with active interrogation.

#### REFERENCES

- 
- <sup>1</sup> O. H. W. Siegmund, A. S. Tremsin, J. V. Vallerga, et al., Nucl. Instr. Meth. A 504 (2003) 177
- <sup>2</sup> A. Vredenburg, W. G. Roeterdink, M. H. M. Janssen, "A photoelectron-photon coincidence imaging apparatus for femtosecond time-resolved molecular dynamics with electron TOF resolution of 18 ps and energy resolution 3.5%", Rev. Sci. Instr., (2008) in print.
- <sup>3</sup> C. P. Beetz, R. W. Boerstler, J. Steinbeck, B. Lemieux, D. R. Winn, Nucl. Instr. Meth. A 442 (2000) 443
- <sup>4</sup> A. W. Smith, C. P. Beetz, R. W. Boerstler, D. R. Winn, and J.W. Steinbeck, Proc. SPIE 4128 (2000) 14.
- <sup>5</sup> O. H. W. Siegmund, A. S. Tremsin, J. V. Vallerga, C. P. Beetz, R. W. Boerstler, D. R. Winn, "Silicon microchannel plates: initial results for photon counting detectors", Proc. SPIE 4140 (2001) 188.
- <sup>6</sup> A. S. Tremsin, J. V. Vallerga, O. H. W. Siegmund, C. P. Beetz and R. W. Boerstler, "Thermal properties of silicon micromachined microchannel plates", Rev. Sci. Instr. 75 (2004) 1068.
- <sup>7</sup> A. Govyadinov, I. Emeliantchik, A. Kurilin, Nucl Instr. Meth. A 419 (1998) 667
- <sup>8</sup> K. Delendik, I. Emeliantchik, A. Litomin, V. Romyantsev, O. Voitik, Nucl. Phys. B (Proc Suppl.) 125 (2003) 394.
- <sup>9</sup> Yi Whikun, et al., Rev. Sci. Instr. 71 (2000) 4165.
- <sup>10</sup> A. Martin, J. Vallerga, J. McPhate, O. Siegmund, Proc SPIE 4854 (2003) 526
- <sup>11</sup> O. Siegmund et al , Nuclear Instruments and Methods in Physics Research A 579 (2007) 188–191
- <sup>12</sup> Paradigm Optics: [www.paradigmoptics.com](http://www.paradigmoptics.com)

**Neal T. Sullivan** is the CTO at Arradance where he has led the development of active thin film materials, processes and technology since 2006. Neal was the Vice President of Technology at Soluris Inc., responsible for the development of several generations of optical and charged particle semiconductor process metrology equipment. Prior to this he was a Principal Engineer in Digital Semiconductor's Advanced Semiconductor Development group. Neal has authored more than 50 publications, is named inventor on 5 US patents, has 6 US patents pending and is the recipient of several industry and academic honors, including a 2004 R&D 100 award.